MATCH
Communications in Mathematical and in Computer Chemistry

MATCH Commun. Math. Comput. Chem. **63** (2010) 3-24

ISSN 0340 - 6253

Correlation Diagrams of Stereoisograms for Characterizing Stereoisomers as Binuclear and Uninuclear Promolecules.

Shinsaku Fujita

Shonan Institute of Chemoinformatics and Mathematical Chemistry

Kaneko 479-7 Ooimachi, Ashigara-Kami-Gun, Kanagawa-Ken, 258-0019

Japan

(Received November 14, 2008)

Abstract

The concept of *correlation diagrams of stereoisograms* has been developed to characterize a set of stereoisomers. Each of the stereoisomers is regarded as a tetrahedral uninuclear promolecule at an *RS*-stereogenic center or a binuclear promolecule at a bond selected to be considered. Stereoisograms, each of which is constructed from a quadruplet of such promolecules according to Fujita's formulation (Fujita, S. *J. Org. Chem.* **2004**, *69*, 3158–3165), are collected to give a correlation diagram at the center or bond. When all of the *RS*-stereogenic centers (along with the bond) are taken into consideration, a set of correlation diagrams are generated to characterize the set of stereoisomers. Because each stereoisogram represents the local chirality/achirality and the local *RS*-stereogenicity/*RS*-astereogenicity of the *RS*-stereogenic center (or the bond), the corresponding correlation diagram indicates total features of such local symmetries. Non-degenerate and degenerate cases having two or four *RS*-stereogenic centers along with a central bond to be considered have been investigated by using correlation diagrams of stereoisograms. Thereby, oversimplified features of the conventional dichotomy between enantiomers and diastereomers have been discussed in detail.

1 Introduction

Although the concept of *stereogenicity* is important to understand stereochemistry (particularly nomenclatures for specifying stereoisomerism), it has not been directly defined in the

IUPAC 1996 Recommendations [1]. In place of the direct definition of the concept, the term "stereogenic unit" has been defined in the IUPAC 1996 recommendations [1] and referred to as "a unit generating stereoisomerism" even in the IUPAC 2004 Provisional Recommendations [2, P-91.1.1.1]. The indirect definition based on the use of the term "stereogenic unit" implies that the IUPAC 1996 Recommendations regards the stereogenicity as local properties around the unit at issue. This implication means that local stereogenicity and global one should be differentiated.

In the conventional stereochemistry, the necessity of differentiating between local stereogenicity and global one has not been discussed thoroughly, but treated in a practical fashion, as found in the treatment of stereoisomeric tartaric acids. When the Cahn-Ingold-Prelog (CIP) system of giving *RS*-descriptors applied to stereoisomeric tartaric acids, we obtain the following combinations: (2*S*,3*S*) and (2*R*,3*R*) for an enantiomeric pair of tartaric acids (**2** and $\overline{\mathbf{2}}$) as well as (2*R*,3*S*) for an achiral tartaric acid (*meso*-tartaric acid, **1**). As found easily, the *RS*-descriptors are concerned with the configurations of respective "stereogenic centers" (or "asymmetric centers" or "chirality centers" as one kind of stereogenic units) so that they do not directly indicate global symmetries (chirality/achirality and stereogenicity/non-stereogenicity) of the tartaric acids. For example, the *R*- or *S*-descriptor of (2*R*,3*S*)-tartaric acid (**1**) specifies the configuration of each stereogenic center and does not directly indicate the global achirality of (2*R*,3*S*)-tartaric acid (**1**).

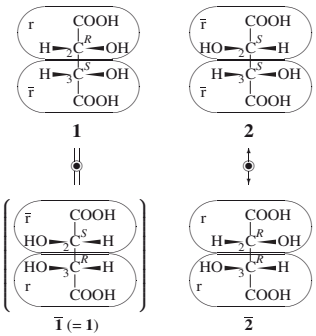

Figure 1: *Meso*-tartaric acid and an enantiomeric pair of chiral tartaric acids. Proligands for correlation diagrams of stereoisograms are designated by r, and r̄.

To demonstrate the achirality of (2*R*,3*S*)-tartaric acid, an appropriate conformation of highest attainable symmetry (e.g., an eclipsed conformation with $\mathbf{C}_s$-symmetry or a staggered conformation with $\mathbf{C}_i$-symmetry) is usually selected [3, pp. 39–41] so that the reflection plane (perpendicular to the C_2—C_3 bond) or the inversion point (at the middle point of the C_2—C_3 bond) is recognized as a source of the achirality (cf. [4]). The stereogenic centers at which the CIP system aims are concluded to have nothing to do with the global symmetry (achirality) of (2*R*,3*S*)-tartaric acid.

The discussion described in the preceding paragraphs shows that we should use the terms *global (local) symmetry*, *global (local) stereogenicity*, and *global (local) chirality* on a more definite basis. As a definite basis of these terms, Fujita [5] has developed the concept of

stereoisograms and indicated that the local stereogenicity related to *RS*-descriptors of the CIP system should be more strictly referred to by the term "local *RS*-stereogenicity" [6, 7]. By means of the concept of *stereoisograms*, the global symmetry of (2*R*,3*S*)-tartaric acid has been shown to be represented by a Type-II stereoisogram, while the local symmetry of the C_2 or C_3 stereogenic center has been characterized by a Type-III-like stereoisogram [5, Fig. 12]. However, the Type-III-like stereoisogram has not been so fully discussed because of its irregular format.

The present paper is devoted to a further advanced basis for the use of the terms *global (local) symmetry*, *global (local) RS-stereogenicity*, and *global (local) chirality*. We here propose the concept of *correlation diagrams of stereoisograms* so that we are able to avoid such an irregular format of stereoisograms in the discussion on the stereochemistry of (2*R*,3*S*)-tartaric acid [5, Fig. 12]. Then, we demonstrate the generality of the concept by using more complicated examples having four stereocenters.

2 Correlation Diagrams of Stereoisograms

2.1 Basic Terminology

According to previous articles [5, 8], we use the symbols listed in Table 1 to indicate the three relationships to draw stereoisograms.

Table 1: Three Relationships and Attributes for Stereoisograms [5, 8]

symbol	relationship	attribute
	enantiomeric	chiral
	(self-enantiomeric)	achiral
	*RS*-diastereomeric	*RS*-stereogenic
	(self-*RS*-diastereomeric)	*RS*-astereogenic
	holantimeric	scleral
	(self-holantimeric)	ascleral

The three relationships correspond to three pairs of attributes for characterizing a promolecule: chiral/achiral, *RS*-stereogenic/*RS*-astereogenic, and scleral/ascleral. As a result, there appears a quadruplet of *RS*-stereoisomers in a stereoisomer, where such *RS*-stereoisomers are categorized into enantiomers, *RS*-diastereomers, and holantimers in accord with the three relationships listed in Table 1. Among eight combinations of the three attributes (Table 1), five types (Type I–V) listed in Table 2 are effective to characterize stereoisograms [5, 8].

2.2 Correlation Diagrams for Two Stereocenters

2.2.1 Characterization of Non-Degenerate Cases

To indicate a non-degenerate case, let us examine stereoisomeric tartaric acid monomethyl esters shown in Fig. 2, which illustrates two enantiomeric pairs: **3**/$\overline{\mathbf{3}}$ and **4**/$\overline{\mathbf{4}}$. When the ligands

Table 2: Five Types of Stereoisograms [5, 8]

Type	combination of the three attributes		
Type I:	chiral	*RS*-stereogenic	ascleral
Type II:	chiral	*RS*-astereogenic	scleral
Type III:	chiral	*RS*-stereogenic	scleral
Type IV:	achiral	*RS*-astereogenic	ascleral
Type V:	achiral	*RS*-stereogenic	scleral

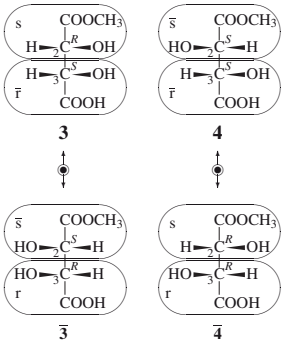

Figure 2: Two enantiomeric pairs of tartaric acid monomethyl esters. Proligands for correlation diagrams of stereoisograms are designated by r, r̄, and so on.

$CH(OH)COOCH_3$ and CH(OH)COOH in **3** are regarded as proligands denoted by the symbols s and r̄, the molecule **3** is represented by a binuclear promolecule r̄—s. Accordingly, its enantiomer $\overline{\mathbf{3}}$ is represented by another binuclear formula r—s̄, where the pairs r/r̄ and s/s̄ denote enantiomeric pairs of proligands in isolation. For the concepts of proligands and promolecules, see [9]. For binuclear promolecules, see [10, 11].

According to [5], the two promolecules r̄—s ($\mathbf{3}_b$) and r—s̄ ($\overline{\mathbf{3}_b}$) construct a stereoisogram of Type II, as shown in Fig. 3(A) (Stereoisogram #1), where the subscript b of $\mathbf{3}_b$ etc. shows that the promolecule at issue is concerned with the central bond of **3** and so on. On a similar line, two promolecules r̄—s̄ ($\mathbf{4}_b$) and r—s ($\overline{\mathbf{4}_b}$) generated from **4** and $\overline{\mathbf{4}}$ construct another stereoisogram of Type II, as also shown in Fig. 3(A) (Stereoisogram #2). The combination of Stereoisograms #1 and #2 is called *a correlation diagram of stereoisograms*. It should be noted that two promolecules of each enantiomeric pair are located in the peripheral positions of the diagram of Fig. 3(A).

Let us next pay attention to C_2 stereocenters of stereoisomers shown in Fig. 3, where four proligands, i.e., OH, $COOCH_3$, r (or r̄), and H, occupy the four positions of a tetrahedral skeleton. The resulting uninuclear promolecules, i.e., $\mathbf{3}_2/\overline{\mathbf{3}_2}$ and $\mathbf{4}_2/\overline{\mathbf{4}_2}$, construct a correlation diagram shown in Fig. 3(B), where the position of each promolecule is selected in accord with the corresponding position of Fig. 3(A) (e.g., $\mathbf{3}_2$ vs. $\mathbf{3}_b$). Note that the subscript 2 corresponds to

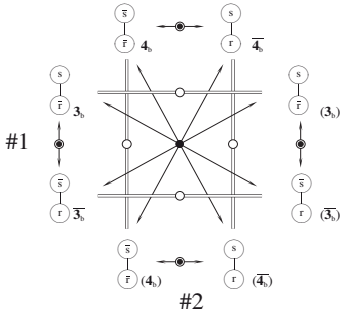

(A) Correlation Diagram at a Central Bond

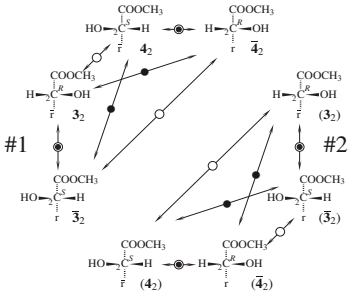

(B) Correlation Diagram at C_2

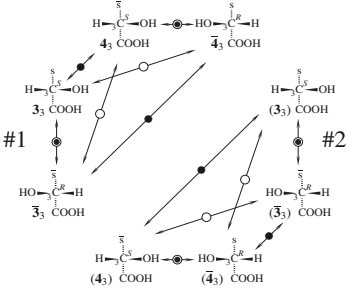

(C) Correlation Diagram at C_3

Figure 3: Correlation diagrams of stereoisograms for stereoisomeric tartaric acid monomethyl esters. (A) For a central bond: Stereoisograms of #1 and #2 both belong to Type II; (B) For C_2: Stereoisograms #1 and #2 are equivalent (Type III), where OH > $COOCH_3$ > r ($\bar{r}$) > H; and (C) For C_3: Stereoisograms #1 and #2 are equivalent (Type III), where OH > COOH > s ($\bar{s}$) > > H.

the C_2 stereocenter. Hence, the uninuclear promolecule $\mathbf{3}_2$ and the binuclear promolecule $\mathbf{3}_b$ represent the same molecule **3**. The four promolecules in the upper left part of Fig. 3(B) ($\mathbf{3}_2/\overline{\mathbf{3}_2}$ and $\mathbf{4}_2/\overline{\mathbf{4}_2}$) construct Stereoisogram #1 of Type III. The four promolecules in the lower right part of Fig. 3(B) ($\mathbf{3}_2/\overline{\mathbf{3}_2}$ and $\mathbf{4}_2/\overline{\mathbf{4}_2}$ all parenthesized) construct Stereoisogram #2 of Type III. Obviously, the two stereoisograms are equivalent so as to be duplicated.

An *RS*-diastereomeric relationship between $\mathbf{3}_2$ and $\mathbf{4}_2$ in Stereoisogram #1 of Type III (Fig. 3(B)) gives a basis to the assignment of *R*- and *S*-descriptors according to the priority sequence, OH > $COOCH_3$ > $\bar{r}$ > H. On the other hand, another *RS*-diastereomeric relationship between $\overline{\mathbf{3}_2}$ and $\overline{\mathbf{4}_2}$ in the same Stereoisogram #1 gives a basis to the assignment of *S*- and *R*-descriptors according to the priority sequence, OH > $COOCH_3$ > r > H. It should be noted that the *R*-configuration of $\mathbf{3}_2$ (due to OH > $COOCH_3$ > $\bar{r}$ > H) is not directly correlated to the *S*-configuration of its enantiomer $\overline{\mathbf{3}_2}$ (due to OH > $COOCH_3$ > r > H) because the priority sequences are different from each other. Although the conventional stereochemistry has con-

sidered $\mathbf{3}_2$ and $\overline{\mathbf{3}_2}$ pairwise in the process of giving *RS*-descriptors, the assignment by pairing such enantiomers is concluded to be only a convention from the present viewpoint. The conventional stereochemistry has overlooked the implicit participation of Stereoisogram #1 of Type III (Fig. 3(B)).

By paying attention to C_3 stereocenters of stereoisomers shown in Fig. 3, we obtain four promolecules, i.e., $\mathbf{3}_3/\overline{\mathbf{3}_3}$ and $\mathbf{4}_3/\overline{\mathbf{4}_3}$, where four proligands, i.e., OH, COOH, s (or $\bar{s}$), and H, occupy the four positions of a tetrahedral skeleton. They construct a correlation diagram shown in Fig. 3(C), where the four promolecules in the upper left part ($\mathbf{3}_3/\overline{\mathbf{3}_3}$ and $\mathbf{4}_3/\overline{\mathbf{4}_3}$) construct Stereoisogram #1 of Type III, while the four promolecules in the lower right part, i.e., $(\mathbf{3}_3)/(\overline{\mathbf{3}_3})$ and $(\mathbf{4}_3)/(\overline{\mathbf{4}_3})$ (all parenthesized), construct Stereoisogram #2 of Type III. Obviously, Stereoisogram #2 is equivalent to #1.

It should be noted that there are other combinations for constructing stereoisograms, i.e., $\mathbf{3}_3/\overline{\mathbf{3}_3}$ and $(\mathbf{4}_3)/(\overline{\mathbf{4}_3})$ at the lower left part of Fig. 3(C); as well as $(\mathbf{3}_3)/(\overline{\mathbf{3}_3})$ and $\mathbf{4}_3/\overline{\mathbf{4}_3}$ at the upper right part. This ambiguity stems from the molecular symmetries of the participant molecules belonging to Type II so that it does not influence discussions and conclusions.

According to an *RS*-diastereomeric relationship between $\mathbf{3}_3$ and $\overline{\mathbf{4}_3}$ in Stereoisogram #1 of Type III (Fig. 3(C)), we are able to assign *S*- and *R*-descriptors (the priority sequence, OH > COOH > s > H). On the other hand, another *RS*-diastereomeric relationship between $\overline{\mathbf{3}_3}$ and $\mathbf{4}_3$ in the same Stereoisogram #1 gives a basis to the assignment of *R*- and *S*-descriptors (the priority sequence, OH > COOH > $\bar{s}$> H). Again, the *S*-configuration of $\mathbf{3}_3$ (due to OH > COOH > s > H) is not directly correlated to the *R*-configuration of its enantiomer $\overline{\mathbf{3}_3}$ (due to OH > COOH > $\bar{s}$ > H) because the priority sequences are different from each other. Although this type of pairing ($\mathbf{3}_3/\overline{\mathbf{3}_3}$) has been a widespread convention for giving *RS*-descriptors, it should be pointed out that such pairing in the conventional stereochemistry again overlooks the implicit participation of Stereoisogram #1 of Type III (Fig. 3(C)).

2.2.2 Characterization of Degenerate Cases

Stereoisomeric tartaric acids (Fig. 1) as a degenerate case can be discussed by modifying the above-mentioned treatment of the non-degenerate case (Figs. 2 and 3). By converting the ligand $COOCH_3$ of the promolecules listed in Fig. 3 into the ligand COOH, we obtain the corresponding correlation diagrams shown in Fig. 4.

The correlation diagram shown in Fig. 4(A) contains two stereoisograms, which are composed of binuclear promolecules. The binuclear promolecule **1** ($\bar{r}$—r), which is superposable to its enantiomer $\overline{\mathbf{1}}$ (r—$\bar{r}$), constructs a stereoisogram of Type IV, which is depicted as Stereoisogram #1 contained in Fig. 4(A). On the other hand, two promolecules $\bar{r}$—$\bar{r}$ ($\mathbf{2}_b$) and r—r ($\overline{\mathbf{2}_b}$) generated from **2** and $\overline{\mathbf{2}}$ construct a stereoisogram of Type II, as shown in Fig. 4(A) (Stereoisogram #2).

When we pay attention to C_2 stereocenters of stereoisomers shown in Fig. 1, we obtain a correlation diagram shown in Fig. 4(B), which contains two stereoisograms (#1 and #2) composed of promolecules $\mathbf{1}_2/\overline{\mathbf{1}_2}$ and of promolecules $\mathbf{4}_2/\overline{\mathbf{4}_2}$. They are equivalent, because the same set of four proligands, i.e., OH, COOH, r (or $\bar{r}$), and H, occupies the four positions of a tetrahedral uninuclear skeleton.

An *RS*-diastereomeric relationship between $\mathbf{1}_2$ and $\mathbf{2}_2$ in Stereoisogram #1 of Type III (Fig. 3(B)) gives a basis to the assignment of *R*- and *S*-descriptors according to the priority sequence, OH > COOH > $\bar{r}$ > H. On the other hand, another *RS*-diastereomeric relationship between $\overline{\mathbf{1}_2}$ (parenthesized) and $\overline{\mathbf{2}_2}$ in the same Stereoisogram #1 gives a basis to the assignment of *S*-

and *R*-descriptors according to the priority sequence, OH > COOH > r > H. It should be emphasized that $\mathbf{1}_2$ and $\overline{\mathbf{1}_2}$ (parenthesized) represent the same achiral molecule **1**. Hence, the different promolecules $\mathbf{1}_2$ and $\overline{\mathbf{1}_2}$ (parenthesized) should be regarded as exhibiting the local symmetry (local chirality and local *RS*-stereogenicity) at the C_2 atom of the achiral molecule **1** in the form of a Type-III stereoisogram.

In contrast, the conventional process assigns an *R*-descriptor to $\mathbf{1}_2$ without considering $\overline{\mathbf{1}_2}$, because $\mathbf{1}_2$ and $\overline{\mathbf{1}_2}$ represent the same achiral molecule **1**. Even if $\mathbf{1}_2$ and $\overline{\mathbf{1}_2}$ were compared in the conventional process, the *R*-configuration of $\mathbf{1}_2$ (due to OH > COOH > $\bar{\text{r}}$ > H) is not directly correlated to the *S*-configuration of its enantiomer $\overline{\mathbf{1}_2}$ (due to OH > COOH > r > H) because the priority sequences are different from each other. The conventional stereochemistry has overlooked the implicit participation of the *RS*-diastereomeric relationship between $\mathbf{1}_2$ and $\mathbf{2}_2$, as found in Stereoisogram #1 of Type III (Fig. 4(B)).

Stereoisogram #1 of Type III (Fig. 4(B)) is alternatively recognized to show the assignment of an *S*-descriptor to the C_2 of **2** by using the *RS*-diastereomeric relationship between $\mathbf{2}_2$ and $\mathbf{1}_2$ as well as the assignment of an *R*-descriptor to the C_2 of $\overline{\mathbf{2}}$ by using *RS*-diastereomeric relationship between $\overline{\mathbf{2}_2}$ and $\overline{\mathbf{1}_2}$ (parenthesized). This methodology is in sharp contrast to the conventional method of stereochemistry in which the *S*-configuration of $\mathbf{2}_2$ is directly correlated to the *R*-configuration of its enantiomer $\overline{\mathbf{2}_2}$ in spite of their different priority sequences (OH > COOH > r > H vs. OH > COOH > $\bar{\text{r}}$ > H).

The C_3 stereocenter of each stereoisomer shown in Fig. 1 accommodates four proligands, i.e., OH, COOH, r (or $\bar{\text{r}}$), and H. The corresponding correlation diagram is shown in Fig. 4(C), which contains two equivalent stereoisograms (#1 and #2). Although we adopt $\mathbf{3}_3/(\overline{\mathbf{3}_3})$ and $\mathbf{4}_3/\overline{\mathbf{4}_3}$ for constructing Stereoisogram #1 (the upper left part), we can alternatively select $\mathbf{3}_3/(\overline{\mathbf{3}_3})$ and $(\mathbf{4}_3)/(\overline{\mathbf{4}_3})$ (parenthesized) at the lower left part of Fig. 4(C). This ambiguity stems from the molecular symmetries of **3** (Type V) and $\mathbf{4}/\overline{\mathbf{4}}$ (Type II) so that it does not influence discussions and conclusions.

Another set of four remaining promolecules at the lower right part of Fig. 3(C), i.e., $(\mathbf{3}_3)/(\overline{\mathbf{3}_3})$ and $(\mathbf{4}_3)/(\overline{\mathbf{4}_3})$ (all parenthesized), construct Stereoisogram #2 of Type III. Obviously, Stereoisogram #2 is equivalent to Stereoisogram #1 because of the molecular symmetries of the participant molecules.

According to an *RS*-diastereomeric relationship between $\mathbf{1}_3$ and $\overline{\mathbf{2}_3}$ in Stereoisogram #1 of Type III (Fig. 3(C)), we are able to assign *S*- and *R*-descriptors (the priority sequence, OH > COOH > r > H). On the other hand, another *RS*-diastereomeric relationship between $\overline{\mathbf{3}_3}$ and $\mathbf{4}_3$ in the same Stereoisogram #1 gives a basis to the assignment of *R*- and *S*-descriptors (the priority sequence, OH > COOH > $\bar{\text{r}}$ > H). Again, the *S*-configuration of the promolecule $\mathbf{1}_3$ (due to OH > COOH > r > H) is not directly correlated to the *R*-configuration of its enantiomeric promolecule $\overline{\mathbf{1}_3}$ (due to OH > COOH > $\bar{\text{s}}$ > H) because the priority sequences are different from each other. It should be noted that the promolecules $\mathbf{1}_3$ and $\overline{\mathbf{1}_3}$ (parenthesized) indicate the local symmetry (local chirality and local *RS*-stereogenicity) at the C_3 stereocenters, although they globally represent the same achiral molecule **1**.

Finally, Stereoisogram #1 of Fig. 3(B) and Stereoisogram #1 of Fig. 3(C) represent equivalent characteristics because of the global symmetries of the participant molecules, which are represented by Fig. 3(A). Even though equivalent, the two stereoisograms distinctly represent the local symmetries at the C_2 and C_3 stereocenters, which should not be confused with the global symmetries represented by Fig. 3(A). In this context, the Type-III-like stereoisogram reported in [5, Fig. 12] should be revised into Stereoisogram #1 of Fig. 3(B) or Stereoisogram #1 of Fig. 3(C), which belong to Type III.

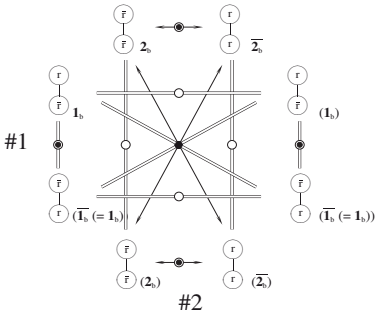

(A) Correlation Diagram at a Central Bond

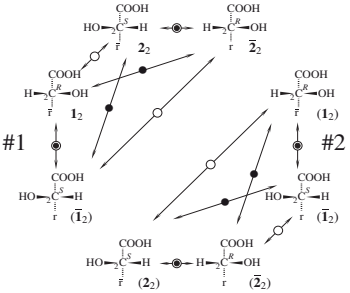

(B) Correlation Diagram at C_2

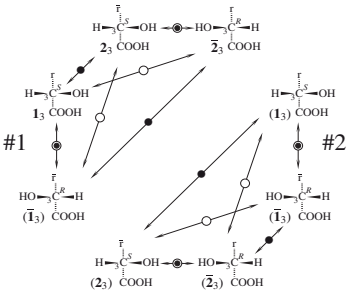

(C) Correlation Diagram at C_3

Figure 4: Correlation diagrams of stereoisograms for stereoisomeric tartaric acids. (A) For a central bond: Stereoisogram of #1 belong to Type IV, while Stereoisogram of #2 belong to Type II; (B) For C_2: Stereoisograms #1 and #2 are equivalent (Type III), where OH $>$ COOH $>$ r ($\bar{\text{r}}$) $>$ H; and (C) For C_3: Stereoisograms #1 and #2 are equivalent (Type III), where OH $>$ COOH $>$ r ($\bar{\text{r}}$) $>$ H.

2.3 Correlation Diagrams for Four Stereocenters

2.3.1 Characterization of Non-Degenerate Cases

The above-mentioned discussions on the cases having two stereocenters can be extended to cases having four stereocenters. By examining Figs. 3 and 4, it is sufficient to select the upper left part of each correlation diagram. In other words, each lower right part involving parenthesized promolecules can be omitted to give a simplified diagram without loosing generality. Because the present cases of four stereoisomers would give huge correlation diagrams, we use such simplified diagrams corresponding to the half parts of respective correlation diagrams. According to this guideline, let us examine eight enantiomeric pairs of 2,3,4,5-tetrahydroxyhexanedioic acid monomethyl esters shown in Fig. 5 as one example of non-degenerate cases.

First, the molecules listed in Fig. 5 are regarded as binuclear promolecules, where each central bond (C_3—C_4) is taken into consideration. By using the symbols r_i ($\bar{r}_i$) and s_i ($\bar{s}_i$)

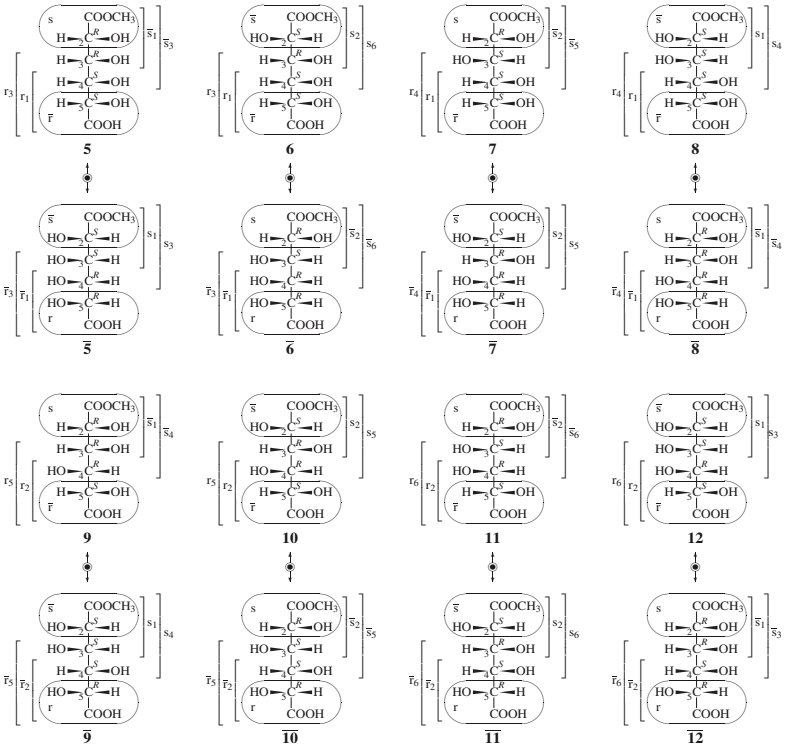

Figure 5: Eight enantiomeric pairs of 2,3,4,5-tetrahydroxyhexanedioic acid monomethyl esters. Proligands for drawing correlation diagrams are designated by letters r, $\bar{\mathrm{r}}$, and so on.

for representing proligands ($i = 1$ and 2), the resulting binuclear promolecules are arranged to construct a correlation diagram of stereoisograms, as shown in Fig. 6(A). Because all of the stereoisograms appearing in Fig. 6(A) belong to Type II, the right part of each stereoisogram is omitted so that respective enantiomeric pairs are depicted at peripheral positions of the correlation diagram (Fig. 6(A)).

The C_2 stereocenter of each stereoisomer shown in Fig. 5 is regarded as being attached by a set of four proligands OH, $COOCH_3$, r_i (or $\bar{\mathrm{r}}_i$), and H, where i = 3–6. The corresponding uninuclear promolecules ($\mathbf{5}_2/\overline{\mathbf{5}}_2$–$\mathbf{12}_2/\overline{\mathbf{12}}_2$) construct a correlation diagram of stereoisograms shown in Fig. 6(B), which involves four stereoisograms (#1–#4) of Type III.

An *RS*-diastereomeric relationship between $\mathbf{5}_2$ and $\mathbf{6}_2$ in Stereoisogram #1 of Type III (Fig. 6(B)) gives a basis to the assignment of *R*- and *S*-descriptors according to the priority sequence, OH > $COOCH_3$ > r_3 > H. On the other hand, another *RS*-diastereomeric relationship between $\overline{\mathbf{5}}_2$ and $\overline{\mathbf{6}}_2$ in the same Stereoisogram #1 gives a basis to the assignment of *S*- and *R*-descriptors according to the priority sequence, OH > $COOCH_3$ > $\bar{\mathrm{r}}_3$ > H.

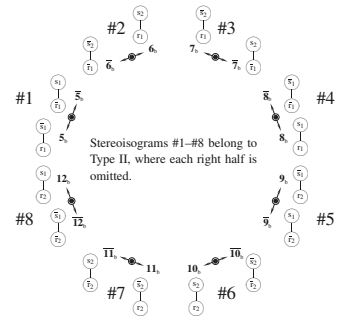

(A) Correlation Diagram at a Central Bond

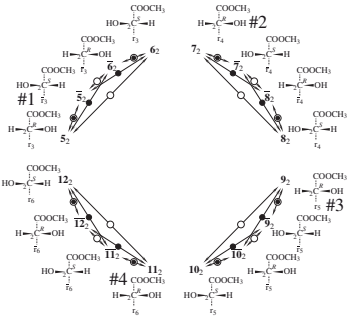

(B) Correlation Diagram at C_2

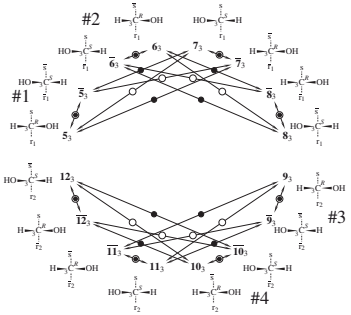

(C) Correlation Diagram at C_3

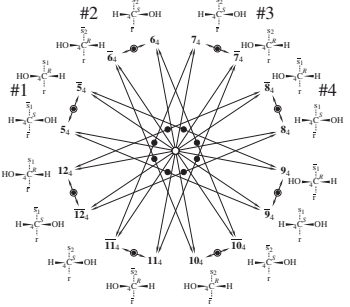

(D) Correlation Diagram at C_4

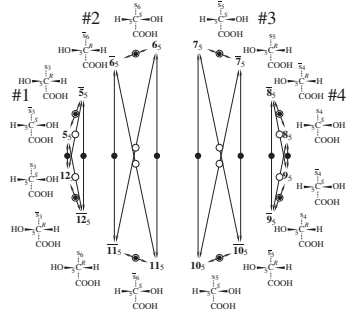

(E) Correlation Diagram at C_5

Figure 6: Correlation diagrams of stereoisograms for stereoisomeric 2,3,4,5-tetrahydroxyhexanedioic acid monomethyl esters. (A) For a central bond: Stereoisogram of #1–#8 belong to Type II; (B) For C_2: Stereoisograms #1–#4 belong to Type III where OH > $COOCH_3$ > r_i ($\overline{r}_i$) > H ($i = 3$–6); (C) For C_3: Stereoisograms #1–#4 belong to Type III, where OH > s ($\overline{s}$) > r_i ($\overline{r}_i$) > H ($i = 1,2$); (D) For C_4: Stereoisograms #1–#4 belong to Type III, where OH > r ($\overline{r}$) > s_i ($\overline{s}_i$) > H ($i = 1,2$); and (D) For C_5: Stereoisograms #1–#4 belong to Type III, where OH > COOH > s_i ($\overline{s}_i$) > H($i = 3$–6).

The correlation diagram shown in Fig. 6(B) contains additional stereoisograms of Type III, i.e., Stereoisogram #2: an *RS*-diastereomeric relationship between $\mathbf{7}_2$ and $\mathbf{8}_2$ (the priority sequence, OH > $COOCH_3$ > r_4 > H) and another *RS*-diastereomeric relationship between $\overline{\mathbf{7}_2}$ and $\overline{\mathbf{8}_2}$ (the priority sequence, OH > $COOCH_3$ > $\bar{r}_4$ > H); Stereoisogram #3: an *RS*-diastereomeric relationship between $\mathbf{9}_2$ and $\mathbf{10}_2$ (the priority sequence, OH > $COOCH_3$ > r_5 > H) and another *RS*-diastereomeric relationship between $\overline{\mathbf{9}_2}$ and $\overline{\mathbf{10}_2}$ (the priority sequence, OH > $COOCH_3$ > $\bar{r}_5$ > H); as well as Stereoisogram #4: an *RS*-diastereomeric relationship between $\mathbf{11}_2$ and $\mathbf{12}_2$ (the priority sequence, OH > $COOCH_3$ > r_6 > H) and another *RS*-diastereomeric relationship between $\overline{\mathbf{11}_2}$ and $\overline{\mathbf{12}_2}$ (the priority sequence, OH > $COOCH_3$ > $\bar{r}_6$ > H). The listed *RS*-diastereomeric relationships are used to give *RS*-descriptors according to the respective priority sequences attached in pairs of parentheses.

The C_3 stereocenters of stereoisomers listed in Fig. 5, each of which is attached by a set of four proligands represented by OH, s ($\bar{s}$), r_i (or $\bar{r}_i$), and H (i = 1 and 2), are characterized by a correlation diagram shown in Fig. 6(C). The correlation diagram involves four stereoisograms (#1–#4) of Type III as follows: Stereoisogram #1: an *RS*-diastereomeric relationship between $\mathbf{5}_3$ and $\mathbf{7}_3$ (the priority sequence, OH > s > r_1 > H) and another *RS*-diastereomeric relationship between $\overline{\mathbf{5}_3}$ and $\overline{\mathbf{7}_3}$ (the priority sequence, OH > $\bar{s}$ > $\bar{r}_1$ > H); Stereoisogram #2: an *RS*-diastereomeric relationship between $\mathbf{6}_3$ and $\mathbf{8}_3$ (the priority sequence, OH > $\bar{s}$ > r_1 > H) and another *RS*-diastereomeric relationship between $\overline{\mathbf{6}_3}$ and $\overline{\mathbf{8}_3}$ (the priority sequence, OH > s > $\bar{r}_1$ > H); Stereoisogram #3: an *RS*-diastereomeric relationship between $\mathbf{9}_3$ and $\mathbf{11}_3$ (the priority sequence, OH > s > r_2 > H) and another *RS*-diastereomeric relationship between $\overline{\mathbf{9}_3}$ and $\overline{\mathbf{11}_3}$ (the priority sequence, OH > $\bar{s}$ > $\bar{r}_2$ > H); as well as Stereoisogram #4: an *RS*-diastereomeric relationship between $\mathbf{10}_3$ and $\mathbf{12}_3$ (the priority sequence, OH > $\bar{s}$ > r_2 > H) and another *RS*-diastereomeric relationship between $\overline{\mathbf{10}_3}$ and $\overline{\mathbf{12}_3}$ (the priority sequence, OH > s > $\bar{r}_2$ > H). The listed *RS*-diastereomeric relationships are used to give *RS*-descriptors according to the respective priority sequences attached in pairs of parentheses.

The C_4 stereocenter of each stereoisomer listed in Fig. 5 is attached by a set of four proligands represented by OH, r ($\bar{r}$), s_i (or $\bar{s}_i$), and H (i = 1 and 2). The corresponding uninuclear promolecules are characterized by a correlation diagram shown in Fig. 6(D), which involves four stereoisograms (#1–#4) of Type III, i.e., Stereoisogram #1: an *RS*-diastereomeric relationship between $\mathbf{5}_4$ and $\mathbf{9}_4$ (the priority sequence, OH > $\bar{r}$> $\bar{s}_1$ > H) and another *RS*-diastereomeric relationship between $\overline{\mathbf{5}_4}$ and $\overline{\mathbf{9}_4}$ (the priority sequence, OH > r > s_1 > H); Stereoisogram #2: an *RS*-diastereomeric relationship between $\mathbf{6}_4$ and $\mathbf{10}_4$ (the priority sequence, OH > $\bar{r}$> s_2 > H) and another *RS*-diastereomeric relationship between $\overline{\mathbf{6}_4}$ and $\overline{\mathbf{10}_4}$ (the priority sequence, OH > r > $\bar{s}_2$ > H); Stereoisogram #3: an *RS*-diastereomeric relationship between $\mathbf{7}_4$ and $\mathbf{11}_4$ (the priority sequence, OH > $\bar{r}$ > $\bar{s}_2$ > H) and another *RS*-diastereomeric relationship between $\overline{\mathbf{7}_4}$ and $\overline{\mathbf{11}_4}$ (the priority sequence, OH > r > s_2 > H); as well as Stereoisogram #4: an *RS*-diastereomeric relationship between $\mathbf{8}_4$ and $\mathbf{12}_4$ (the priority sequence, OH > $\bar{r}$> s_1 > H) and another *RS*-diastereomeric relationship between $\overline{\mathbf{8}_4}$ and $\overline{\mathbf{12}_4}$ (the priority sequence, OH > r > $\bar{s}_1$ > H). The listed *RS*-diastereomeric relationships are used to give *RS*-descriptors according to the respective priority sequences attached in pairs of parentheses.

Each C_5 stereocenter of the stereoisomers shown in Fig. 5 is attached by a set of four proligands represented by OH, COOH, s_i (or $\bar{s}_i$), and H, where i = 3–6. The resulting uninuclear promolecules ($\mathbf{5}_5/\overline{\mathbf{5}_5}$–$\mathbf{12}_5/\overline{\mathbf{12}_5}$) construct a correlation diagram of stereoisograms shown in Fig. 6(D), which involves four stereoisograms (#1–#4) of Type III. The following *RS*-diastereomeric relationships in respective stereoisograms are used to give *RS*-descriptors according to priority sequences attached in pairs of parentheses, i.e., Stereoisogram #1: an *RS*-diastereomeric re-

lationship between $\mathbf{5}_5$ and $\overline{\mathbf{12}_5}$ (the priority sequence, OH > COOH > $\bar{s}_3$ > H) and another *RS*-diastereomeric relationship between $\overline{\mathbf{5}_5}$ and $\mathbf{12}_5$ (the priority sequence, OH > COOH > s_3 > H); Stereoisogram #2: an *RS*-diastereomeric relationship between $\mathbf{6}_5$ and $\overline{\mathbf{11}_5}$ (the priority sequence, OH > COOH > s_6 > H) and another *RS*-diastereomeric relationship between $\overline{\mathbf{6}_5}$ and $\mathbf{11}_5$ (the priority sequence, OH > COOH > $\bar{s}_6$ > H); Stereoisogram #3: an *RS*-diastereomeric relationship between $\mathbf{7}_5$ and $\overline{\mathbf{10}_5}$ (the priority sequence, OH > COOH > $\bar{s}_5$ > H) and another *RS*-diastereomeric relationship between $\overline{\mathbf{7}_5}$ and $\mathbf{10}_5$ (the priority sequence, OH > COOH > s_5 > H); as well as Stereoisogram #4: an *RS*-diastereomeric relationship between $\mathbf{8}_5$ and $\overline{\mathbf{9}_5}$ (the priority sequence, OH > COOH > s_4 > H) and another *RS*-diastereomeric relationship between $\overline{\mathbf{8}_5}$ and $\mathbf{9}_5$ (the priority sequence, OH > COOH > $\bar{s}_4$ > H).

2.3.2 Characterization of Degenerate Cases

A degenerate case of stereoisomeric 2,3,4,5-tetramethylhexanedioic acids (Fig. 7) can be discussed in comparing with the above-mentioned non-degenerate case of their monomethyl esters (Fig. 5). Each molecule listed in Fig. 7 is obtained by converting the ligand $COOCH_3$ of the monomethyl ester (occupying the corresponding position of Fig. 5) into the ligand COOH. Thereby, there appear two achiral molecules (**13** and **19**) and four pairs of enantiomers (**14**/$\overline{\mathbf{14}}$, **15**/$\overline{\mathbf{15}}$, **16**/$\overline{\mathbf{16}}$, and **18**/$\overline{\mathbf{18}}$). Degenerate features are characterized by the presence of two superposable mirror images ($\overline{\mathbf{13}}$ and $\overline{\mathbf{19}}$ parenthesized to exhibit duplication) and by the presence of two parenthesized (duplicated) pairs of enantiomers (**17**/$\overline{\mathbf{17}}$ and **20**/$\overline{\mathbf{20}}$).

When we pay attention to the central bonds (C_3—C_4) of respective molecules listed in Fig. 7, the corresponding binuclear promolecules construct a correlation diagram shown in Fig. 8(A), where two proligands selected from r_1 ($\bar{r}_1$) and r_2 ($\bar{r}_2$) are linked to generate each binuclear promolecule. Stereoisograms #1 (r_1—$\bar{r}_1$) and #6 (r_2—$\bar{r}_2$) belong to Type IV, which shows the *meso*-characters of **13** and **19**. On the other hand, Stereoisograms #2–#5 belong to Type II.

In accord with the degenerate nature of the correlation diagram shown in Fig. 8(A), parenthesized Stereoisograms #2 is equivalent to Stereoisograms #2; and parenthesized Stereoisograms #3 is also equivalent to Stereoisograms #3. In spite of duplication, these stereoisograms are necessary to go on with the following discussions on other correlation diagrams.

The C_2 stereocenter of each stereoisomer shown in Fig. 7 is attached by a set of four proligands represented by OH, COOH, r_i (or $\bar{r}_i$), and H, where i = 3–6. The corresponding uninuclear promolecules construct a correlation diagram of stereoisograms shown in Fig. 8(B), which involves four stereoisograms (#1–#4) of Type III.

Although the pair of **17**/$\overline{\mathbf{17}}$ (parenthesized) is identical to the pair **15**/$\overline{\mathbf{15}}$, the corresponding pair of promolecules $\mathbf{17}_2$/$\overline{\mathbf{17}_2}$ (parenthesized) is different from the pair of promolecules $\mathbf{15}_2$/$\overline{\mathbf{15}_2}$. This means that the local symmetry (local chirality and local *RS*-stereogenicity) at the C_2 atom (Fig. 8(B)) is different from the global symmetry represented by the correlation diagram shown Fig. 8(A). A similar situation holds true for $\mathbf{20}_2$/$\overline{\mathbf{20}_2}$ (parenthesized) vs. $\mathbf{14}_2$/$\overline{\mathbf{14}_2}$.

The four stereoisograms contained in Fig. 8(B) are capable of giving *RS*-descriptors by means of *RS*-diastereomeric relationships, i.e., Stereoisogram #1: an *RS*-diastereomeric relationship between $\mathbf{13}_2$ and $\mathbf{14}_2$ (the priority sequence, OH > COOH > r_3 > H) and another *RS*-diastereomeric relationship between ($\overline{\mathbf{13}_2}$) and $\overline{\mathbf{14}_2}$ (the priority sequence, OH > COOH > $\bar{r}_3$ > H); Stereoisogram #2: an *RS*-diastereomeric relationship between $\mathbf{15}_2$ and $\mathbf{16}_2$ (the priority sequence, OH > COOH > r_4 > H) and another *RS*-diastereomeric relationship between $\overline{\mathbf{15}_2}$ and $\overline{\mathbf{16}_2}$ (the priority sequence, OH > COOH > $\bar{r}_4$ > H); Stereoisogram #3: an *RS*-diastereomeric relationship between ($\mathbf{17}_2$) and $\mathbf{18}_2$ (the priority sequence, OH > COOH > r_5 > H) and another

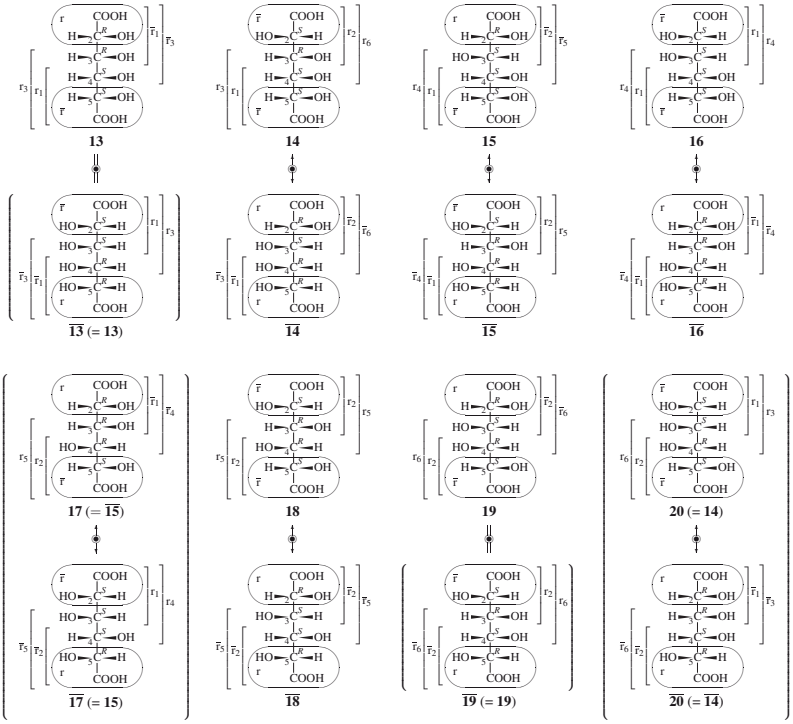

Figure 7: Six (self-)enantiomeric pairs of 2,3,4,5-tetrahydroxyhexanedioic acids. Proligands for drawing correlation diagrams are designated by letters r, $\bar{r}$, and so on. Each parenthesized molecule (or pair) is duplicated because locant numbers are not taken into consideration.

RS-diastereomeric relationship between ($\overline{\mathbf{17}_2}$) and $\overline{\mathbf{18}_2}$ (the priority sequence, OH > COOH > $\bar{r}_5$ > H); Stereoisogram #4: an *RS*-diastereomeric relationship between $\mathbf{19}_2$ and ($\mathbf{20}_2$) (the priority sequence, OH > COOH > r_6 > H) and another *RS*-diastereomeric relationship between $\overline{\mathbf{19}_2}$ and ($\overline{\mathbf{20}_2}$) (the priority sequence, OH > COOH > $\bar{r}_6$ > H).

The C_3 stereocenter of each stereoisomer listed in Fig. 7 is attached by a set of four proligands represented by OH, r ($\bar{r}$), r_i (or $\bar{r}_i$), and H (i = 1 and 2). The corresponding uninuclear promolecules are characterized by a correlation diagram shown in Fig. 8(C), which involves four stereoisograms (#1–#4) of Type III. Each stereoisogram contains two *RS*-Diastereomeric relationships, which are used to give *RS*-descriptors according to the respective priority sequences attached in pairs of parentheses, i.e., Stereoisogram #1: an *RS*-diastereomeric relationship between $\mathbf{13}_3$ and $\mathbf{15}_3$ (the priority sequence, OH > r > r_1 > H) and another *RS*-diastereomeric relationship between $\overline{\mathbf{13}_3}$ and $\overline{\mathbf{15}_3}$ (the priority sequence, OH > $\bar{r}$ > $\bar{r}_1$ > H); Stereoisogram #2: an *RS*-diastereomeric relationship between $\mathbf{14}_3$ and $\mathbf{16}_3$ (the priority sequence, OH > r > $\bar{r}_1$ > H) and another *RS*-diastereomeric relationship between $\overline{\mathbf{14}_3}$ and $\overline{\mathbf{16}_3}$ (the priority sequence, OH

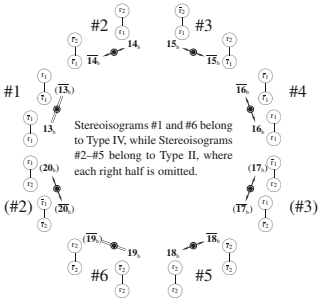

(A) Correlation Diagram at a Central Bond

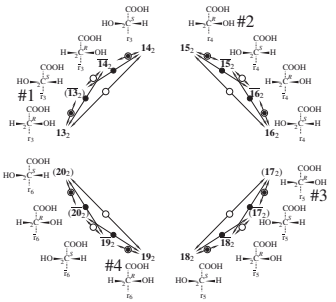

(B) Correlation Diagram at C_2

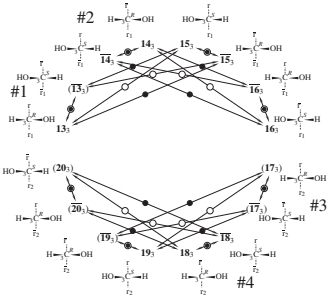

(C) Correlation Diagram at C_3

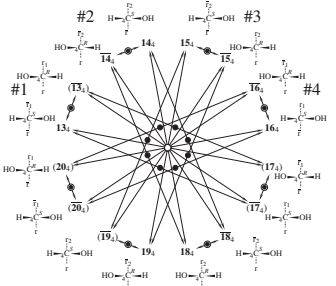

(D) Correlation Diagram at C_4

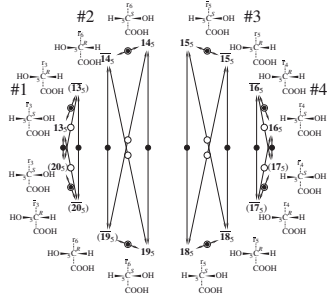

(E) Correlation Diagram at C_5

Figure 8: Correlation diagrams of stereoisograms for stereoisomeric 2,3,4,5-tetrahydroxyhexanedioic acids. (A) For a central bond: Stereoisogram of #2–#5 belong to Type II, while #1 and #6 belong to Type IV; (B) For C_2: Stereoisograms #1–#4 belong to Type III where OH > COOH > r$_i$ ($\bar{\text{r}}_i$) > H (i = 3–6); (C) For C_3: Stereoisograms #1–#4 belong to Type III, where OH > r ($\bar{\text{r}}$) > r$_i$ ($\bar{\text{r}}_i$) > H ($i = 1, 2$); (D) For C_4: Stereoisograms #1–#4 belong to Type III, where OH > r ($\bar{\text{r}}$) > r$_i$ ($\bar{\text{r}}_i$) > H ($i = 1, 2$); and (D) For C_5: Stereoisograms #1–#4 belong to Type III, where OH > COOH > r$_i$ ($\bar{\text{r}}_i$) > H(i = 3–6).

$> \bar{r} > r_1 >$ H); Stereoisogram #3: an *RS*-diastereomeric relationship between (**17**$_3$) and **19**$_3$ (the priority sequence, OH $>$ r $> r_2 >$ H) and another *RS*-diastereomeric relationship between ($\overline{\mathbf{17}_3}$) and ($\overline{\mathbf{19}_3}$) (the priority sequence, OH $> \bar{r} > \bar{r}_2 >$ H); Stereoisogram #4: an *RS*-diastereomeric relationship between **18**$_3$ and (**20**$_3$) (the priority sequence, OH $> \bar{r} > r_2 >$ H) and another *RS*-diastereomeric relationship between $\overline{\mathbf{18}_3}$ and ($\overline{\mathbf{20}_3}$) (the priority sequence, OH $>$ r $> \bar{r}_2 >$ H);

The C_4 stereocenter of each stereoisomer listed in Fig. 7 produces the corresponding uninuclear promolecule shown in Fig. 8(D), where a set of four proligands OH, r ($\bar{r}$), r_i (or $\bar{r}_i$), and H (i = 1 and 2) is taken into consideration. The correlation diagram (Fig. 8(D)) involves four stereoisograms (#1–#4) of Type III, i.e., Stereoisogram #1: an *RS*-diastereomeric relationship between **13**$_4$ and (**17**$_4$) (the priority sequence, OH $> \bar{r} > \bar{r}_1 >$ H) and another *RS*-diastereomeric relationship between ($\overline{\mathbf{13}_4}$) and ($\overline{\mathbf{17}_4}$) (the priority sequence, OH $>$ r $> r_1 >$ H); Stereoisogram #2: an *RS*-diastereomeric relationship between **14**$_4$ and **18**$_4$ (the priority sequence, OH $> \bar{r} > r_2$ $>$ H) and another *RS*-diastereomeric relationship between $\overline{\mathbf{14}_4}$ and $\overline{\mathbf{18}_4}$ (the priority sequence, OH $>$ r $> \bar{r}_2 >$ H); Stereoisogram #3: an *RS*-diastereomeric relationship between **15**$_4$ and **19**$_4$ (the priority sequence, OH $> \bar{r} > \bar{r}_2 >$ H) and another *RS*-diastereomeric relationship between $\overline{\mathbf{15}_4}$ and ($\overline{\mathbf{19}_4}$) (the priority sequence, OH $>$ r $> r_2 >$ H); as well as Stereoisogram #4: an *RS*-diastereomeric relationship between **16**$_4$ and (**20**$_4$) (the priority sequence, OH $> \bar{r} > r_1 >$ H) and another *RS*-diastereomeric relationship between $\overline{\mathbf{16}_4}$ and ($\overline{\mathbf{20}_4}$) (the priority sequence, OH $>$ r $> \bar{r}_1 >$ H). The listed *RS*-diastereomeric relationships are used to give *RS*-descriptors by adopting the respective priority sequences attached in pairs of parentheses.

The correlation diagram shown in Fig. 8(E) is concerned with the C_5 stereocenters of stereoisomers shown in Fig. 7, where each C_5 stereocenter is attached by a set of four proligands represented by OH, COOH, r_i (or $\bar{r}_i$), and H, where i = 3–6. The correlation diagram (Fig. 8(E)) involves four stereoisograms (#1–#4) of Type III, where the following *RS*-diastereomeric relationships in respective stereoisograms are used to give *RS*-descriptors according to priority sequences attached in pairs of parentheses, i.e., Stereoisogram #1: an *RS*-diastereomeric relationship between **13**$_5$ and ($\overline{\mathbf{20}_5}$) (the priority sequence, OH $>$ COOH $> \bar{r}_3 >$ H) and another *RS*-diastereomeric relationship between $\overline{\mathbf{13}_5}$ and **20**$_5$ (the priority sequence, OH $>$ COOH $> r_3$ $>$ H); Stereoisogram #2: an *RS*-diastereomeric relationship between **14**$_5$ and ($\overline{\mathbf{19}_5}$) (the priority sequence, OH $>$ COOH $> r_6 >$ H) and another *RS*-diastereomeric relationship between $\overline{\mathbf{14}_5}$ and **19**$_5$ (the priority sequence, OH $>$ COOH $> \bar{r}_6 >$ H); Stereoisogram #3: an *RS*-diastereomeric relationship between **15**$_5$ and $\overline{\mathbf{18}_5}$ (the priority sequence, OH $>$ COOH $> \bar{r}_5 >$ H) and another *RS*-diastereomeric relationship between $\overline{\mathbf{15}_5}$ and **18**$_5$ (the priority sequence, OH $>$ COOH $> r_5$ $>$ H); as well as Stereoisogram #4: an *RS*-diastereomeric relationship between **16**$_5$ and ($\overline{\mathbf{17}_5}$) (the priority sequence, OH $>$ COOH $> r_4 >$ H) and another *RS*-diastereomeric relationship between $\overline{\mathbf{16}_5}$ and **17**$_5$ (the priority sequence, OH $>$ COOH $> \bar{r}_4 >$ H).

3 Discussion

3.1 Global and Local Symmetries

In the present approach, a local symmetry in a molecule is divided into a local *RS*-stereogenicity (paired with *RS*-astereogenicity) and a local chirality (paired with achirality), where the local *RS*-stereogenicity is a basis for giving *RS*-descriptors of the CIP system. In a parallel way, a global symmetry is divided into a global *RS*-stereogenicity (paired with *RS*-astereogenicity) and a global chirality (paired with achirality). The crux of the present approach is that such local

symmetries at respective sites (stereocenters, bonds, etc.) are characterized by stereoisograms, each of which contains *RS*-stereoisomers concerning the site at issue.

The newly-developed concept *a correlation diagram of stereoisograms* provides us with an integrated perspective over geometrical and stereoisomeric properties characterizing a set of stereoisomers. When we repeatedly compare a correlation diagram constructed at a site of a common locant number of each stereoisomer with a correlation diagram constructed at a site of another common locant number, we find that a correlation diagram of stereoisograms at an appropriate site (i.e., a definitely determined site under an appropriate criterion such as centroids and bicentroids) is found to specify a local symmetry at the site as well as the global symmetry of each stereoisomer. This feature is particularly useful for the characterization of *meso*-molecules.

For example, the correlation diagram of Fig. 4(A) determines the local symmetry at the C_2—C_3 bond of **1** (as the binuclear promolecule $\mathbf{1}_b$) and the local symmetry at the C_2—C_3 bond of $\mathbf{2/\overline{2}}$ (as a pair of promolecules $\mathbf{2}_b/\overline{\mathbf{2}}_b$); at the same time, the binuclear promolecule $\mathbf{1}_b$ (or the pair of binuclear promolecules $\mathbf{2}_b/\ \overline{\mathbf{2}}_b$) indicates the global symmetry of **1** (or $\mathbf{2/\overline{2}}$).

On the other hand, the correlation diagram of Fig. 4(B) indicates the local symmetry at the C_2 stereocenter of **1** (in terms of the uninuclear promolecule $\mathbf{1}_2$) and the local symmetry at the C_2 stereocenter of $\mathbf{2/\overline{2}}$ (in terms of a pair of uninuclear promolecules $\mathbf{2}_2/\overline{\mathbf{2}}_2$). Obviously, the uninuclear promolecules are incapable of representing global symmetries. Parallel situations hold true for the correlation diagram of Fig. 4(C) which determines the local symmetries at the C_3 stereocenters.

Figure 8 shows another example of linking local and global symmetries together. Stereoisogram #1 of Fig. 8(A) indicates the local symmetry at the C_3—C_4 bond of **13** (as the binuclear promolecule $\mathbf{13}_b$) and at the same time the global symmetry of **13**. The Type-IV nature (cf. Table 2) of the binuclear promolecule $\mathbf{13}_b$ corresponds to the fact that **13** is achiral and *RS*-astereogenic globally as determined to be a binuclear *meso*-molecule. This holds true for the promolecule $\mathbf{19}_b$, which also exhibits *meso*-nature. Other correlation diagrams of Fig. 8(A) belong to Type II and show local symmetries at the C_3—C_4 bonds as well as global symmetries.

The correlation diagram of Fig. 4(B) indicates the local symmetry at the C_2 stereocenter of **13** etc. in terms of the uninuclear promolecule $\mathbf{1}_2$ etc., as found in Stereoisogram #1 and so on. However, the uninuclear promolecule $\mathbf{1}_2$ etc. are generally incapable of representing global symmetries. The enantiomeric relationship between $\mathbf{1}_2$ and $(\overline{\mathbf{1}_2})$ is incapable of representing the global symmetry (the global achirality), although it demonstrates the local chirality of **13** well. Parallel situations hold true for the correlation diagrams of Fig. 4(C), (D), and (E), which are concerned with the C_3, C_4, and C_5 stereocenters.

3.2 Balanced and Unbalanced Binuclear Molecules

The dichotomy between centroidal and bicentroidal trees (alkanes as graphs) which was formulated by Jordan [12] and Cayley [13] has been extended to apply to three-dimensional (3D) trees (alkanes as stereoisomers) by Fujita [14, 15]. Thus, 3D trees (alkanes as stereoisomers) were categorized into centroidal and bicentroidal 3D trees as models of acyclic stereoisomers [14, 15]; and then they were enumerated [14, 15] by means of Fujita's proligand method [16, 17, 18]. Alternatively, such 3D trees (alkanes) have been categorized into balanced and unbalanced 3D trees according to another dichotomy developed by Fujita [19]. They were enumerated according to this dichotomy also by employing Fujita's proligand method. A further scheme for enumerating alkanes after dual recognition as uninuclear and binuclear pro-

molecules has been reported by Fujita [11]. Note that a bicentroid is selected from a set of binuclei and that a centroid is selected from a set of uninuclei.

The two dichotomies have been combined to give three categories, i.e., centroidal & unbalanced 3D-trees (alkanes), bicentroidal & unbalanced 3D-trees (alkanes), and bicentroidal & balanced 3D-trees (alkanes) [19]. In this context, we can say that the present paper deals with bicentroidal & unbalanced acyclic stereoisomers (cf. non-degenerate cases) and bicentroidal & balanced acyclic stereoisomers (cf. degenerate cases).

For example, the correlation diagram of Fig. 4(A) indicates that the promolecule $\mathbf{1}_b$ represents a bicentroidal & balanced molecule; and that the pair of promolecules $\mathbf{2}_b/\overline{\mathbf{2}}_b$ also represents a bicentroidal & balanced molecule. The correlation diagram of Fig. 8(A) indicates that the promolecules $\mathbf{13}_b$ and $\mathbf{19}_b$ represent bicentroidal & balanced molecules. The pair of promolecules $\mathbf{16}_b/\overline{\mathbf{16}}_b$ and the pair of promolecules $\mathbf{18}_b/\overline{\mathbf{18}}_b$ represent bicentroidal & balanced molecules. It should be pointed that the balanced nature requires binuclear formulas listed in Fig. 4(A) and Fig. 8(A), because Fig. 4(B) and (C) as well as Fig. 8(B)–(E) are insufficient to discuss geometric and stereoisomeric features, especially global ones.

The remaining promolecules in Fig. 4(A) and Fig. 8(A) are bicentroidal & unbalanced molecules. The unbalanced nature does not necessarily require binuclear formulas listed in Fig. 4(A) and Fig. 8(A), because uninuclear formulas shown in Fig. 4(B) and (C) as well as in Fig. 8(B)–(E) are sufficient to discuss geometric and stereoisomeric features.

Moreover, all of the promolecules listed in in Fig. 3(A) and Fig. 6(A) are bicentroidal & unbalanced molecules. The unbalanced nature does not necessarily require binuclear formulas listed in Fig. 3(A) and Fig. 6(A), because uninuclear formulas shown in Fig. 3(B) and (C) as well as in Fig. 6(B)–(E) are sufficient to discuss geometric and stereoisomeric features.

In summary, the dichotomy between balanced and unbalanced 3D trees (as models of acyclic stereoisomers) is important to discuss global symmetries of the 3D trees. The global symmetries of unbalanced 3D trees can be discussed by means of uninuclear promolecules whether they are centroidal or bicentroidal. Thus, examination of binuclear promolecules is not always required. In contrast, the global symmetries of balanced 3D trees (which are all bicentroidal) should be discussed by means of binuclear promolecules.

3.3 A Remedy for the Over-Simplified Dichotomy

The traditional terminology of stereochemistry has heavily depended on the dichotomy between enantiomeric and diastereomeric relationships, as found in reviews [20, 21], textbooks on stereochemistry [3,22–25], glossaries [1, 2], and several reports on a flow-chart approach [20,26–28]. The dichotomy would be effective for characterizing the stereoisomers shown in Figs. 1 and 2, where they have two stereocenters. However, the cases of four stereocenters shown in Figs. 5 and 7 become less controllable because of over-simplified features of the dichotomy. The dichotomy has been critically discussed by Fujita, where the concepts of *RS*-stereoisomerism and stereoisograms were developed to change the dichotomy into a new theoretical framework [5,7, 29–32]. Such over-simplified features of the conventional dichotomy can be more thoroughly avoided by means of the present concept *correlation diagrams of stereoisograms*.

When the molecule **5** (Fig. 5) is given, for example, we can recognize a pair of enantiomers $\mathbf{5}/\overline{\mathbf{5}}$. According to the dichotomy between enantiomers and diastereomers, the relationship between **5** and **6** is diastereomeric; the relationship between **5** and **7** is also diastereomeric; …; **5** and **12** is also diastereomeric; and **5** and $\overline{\mathbf{12}}$ is also diastereomeric. Thus, the resulting 14 relationships concerning **5** are all determined to be diastereomeric. In general, there appear one

Table 3: Correlation of **5** to *RS*-Stereoisomers

Main correlation diagram		Epimeric correlation diagrams	
Stereoisogram	Quadruplet	Stereoisogram	Quadruplet
Fig. 6(C) #1	$\mathbf{5}_3/\overline{\mathbf{5}}_3$; $\mathbf{7}_3/\overline{\mathbf{7}}_3$		
Fig. 6(C) #2	$\mathbf{6}_3/\overline{\mathbf{6}}_3$; $\mathbf{8}_3/\overline{\mathbf{8}}_3$	Fig. 6(B) #1	$\mathbf{5}_2/\overline{\mathbf{5}}_2$; $\mathbf{6}_2/\overline{\mathbf{6}}_2$
Fig. 6(C) #3	$\mathbf{9}_3/\overline{\mathbf{9}}_3$; $\mathbf{11}_3/\overline{\mathbf{11}}_3$	Fig. 6(D) #1	$\mathbf{5}_4/\overline{\mathbf{5}}_4$; $\mathbf{9}_4/\overline{\mathbf{9}}_4$
Fig. 6(C) #4	$\mathbf{10}_3/\overline{\mathbf{10}}_3$; $\mathbf{12}_3/\overline{\mathbf{12}}_3$	Fig. 6(E) #1	$\mathbf{5}_5/\overline{\mathbf{5}}_5$; $\mathbf{12}_5/\overline{\mathbf{12}}_5$

enantiomer (e.g., $\overline{\mathbf{5}}$) and 14 diastereomers (others listed in Fig. 5) even when the a molecule (e.g., **5**) is fixed to be examined.

The correlation diagrams collected in Fig. 6 provides us with a clue for categorizing 14 diastereomeric relationships appearing in Fig. 5. For the sake of convenience, each pair of enantiomers is taken into consideration. We start from the pair $\mathbf{5}/\overline{\mathbf{5}}$, where the corresponding promolecules at the C_3 stereocenters are contained in Stereoisogram #1 of Fig. 6(C). Note that stereoisograms of Fig. 6(C) is diagrammatic expressions of epimerizations at C_3 atom. Hence, the epimerization of the pair $\mathbf{5}_3/\overline{\mathbf{5}}_3$ into the pair $\mathbf{7}_3/\overline{\mathbf{7}}_3$ appears as the *RS*-diastereomeric relationships in Stereoisogram #1 of Fig. 6(C), as collected in Table 3. By omitting the subscript of each structure number, this epimerization concerning promolecules can be regarded as the C_3-epimerization of the corresponding pairs of molecules, i.e., the pair $\mathbf{5}/\overline{\mathbf{5}}$ converted into the pair $\mathbf{7}/\overline{\mathbf{7}}$.

On a similar line, Stereoisogram #1 of Fig. 6(B), Stereoisogram #1 of Fig. 6(D), and Stereoisogram #1 of Fig. 6(E) represent epimerizations of the pair $\mathbf{5}/\overline{\mathbf{5}}$ into $\mathbf{6}/\overline{\mathbf{6}}$, $\mathbf{9}/\overline{\mathbf{9}}$, and $\mathbf{12}/\overline{\mathbf{12}}$ respectively, as collected in the right column of Table 3. As a result, conventional diastereomeric relationships can be detailedly reinterpreted by means of *RS*-diastereomeric and holantimeric relationships, which are contained in each stereoisogram.

Although diastereomeric relationships between $\mathbf{5}/\overline{\mathbf{5}}$ and the remaining molecules ($\mathbf{8}/\overline{\mathbf{8}}$, $\mathbf{10}/\overline{\mathbf{10}}$, and $\mathbf{11}/\overline{\mathbf{11}}$) cannot be determined by direct epimerizations, they can be traced by multiple epimerization processes. The combination of Stereoisogram #1 of Fig. 6(B) with Stereoisogram #2 of Fig. 6(C) results in a multiple epimerization process: $\mathbf{5}_2/\overline{\mathbf{5}}_2 \rightarrow \mathbf{6}_2/\overline{\mathbf{6}}_2 \rightarrow \mathbf{8}_3/\overline{\mathbf{8}}_3$ (the second row of Table 3). This process is recognized to specify detailed versions of the conventional diastereomeric relationships between **5** and **8** and between **5** and $\overline{\mathbf{8}}$. Similarly, the combination of Stereoisogram #1 of Fig. 6(D) with Stereoisogram #3 of Fig. 6(C) results in a multiple epimerization process: $\mathbf{5}_2/\overline{\mathbf{5}}_2 \rightarrow \mathbf{9}_2/\overline{\mathbf{9}}_2 \rightarrow \mathbf{11}_3/\overline{\mathbf{11}}_3$ (the third row of Table 3); as well as the combination of Stereoisogram #1 of Fig. 6(E) with Stereoisogram #4 of Fig. 6(C) results in a multiple epimerization process: $\mathbf{5}_2/\overline{\mathbf{5}}_2 \rightarrow \mathbf{12}_2/\overline{\mathbf{12}}_2 \rightarrow \mathbf{10}_3/\overline{\mathbf{10}}_3$ (the fourth row of Table 3).

By scrutinizing Table 3, we are able to reach a new viewpoint for selecting multiple epimerization processes. The counterpart stereoisograms which have been combined with the stereoisograms of direct epimerizations all appear in the correlation diagram of Fig. 6(C), which is referred to as *a main correlation diagram* in Table 3. The stereoisogram corresponding to the first direct epimerization is contained in the main correlation diagram (Fig. 6(C)), while the stereoisograms corresponding to the other direct epimerizations are separately contained in the other correlation diagrams named *epimeric correlation diagrams* (Fig. 6(B), (D), and (E)).

In general, an indirect conversion (e.g., **5**→**8**) can be interpreted by a multiple process of

Table 4: Fourteen Diastereomeric Relationships Concerning **5**

Pair	Relationship	Stereoisogram
one enantiomeric relationship		
5/$\overline{\mathbf{5}}$	enantiomeric at C_3	Fig. 6(C) #1
fourteen diastereomeric relationships		
5/7	*RS*-diastereomeric at C_3	Fig. 6(C) #1
5/$\overline{\mathbf{7}}$	holantimeric at C_3	Fig. 6(C) #1
5/6	*RS*-diastereomeric at C_2	Fig. 6(B) #1
5/$\overline{\mathbf{6}}$	holantimeric at C_2	Fig. 6(B) #1
5/8	*RS*-diastereomeric at C_2	Fig. 6(B) #1
	and *RS*-diastereomeric at C_3	Fig. 6(C) #2
5/$\overline{\mathbf{8}}$	*RS*-diastereomeric at C_2	Fig. 6(B) #1
	and holantimeric at C_3	Fig. 6(C) #2
5/9	*RS*-diastereomeric at C_4	Fig. 6(D) #1
5/$\overline{\mathbf{9}}$	holantimeric at C_4	Fig. 6(D) #1
5/11	*RS*-diastereomeric at C_4	Fig. 6(D) #1
	and *RS*-diastereomeric at C_3	Fig. 6(C) #3
5/$\overline{\mathbf{11}}$	*RS*-diastereomeric at C_4	Fig. 6(D) #1
	and holantimeric at C_3	Fig. 6(C) #3
5/12	holantimeric at C_5	Fig. 6(E) #1
5/$\overline{\mathbf{12}}$	*RS*-diastereomeric at C_5	Fig. 6(E) #1
5/10	*RS*-diastereomeric at C_5	Fig. 6(E) #1
	and holantimeric at C_3	Fig. 6(C) #4
5/$\overline{\mathbf{10}}$	*RS*-diastereomeric at C_5	Fig. 6(E) #1
	and *RS*-diastereomeric at C_3	Fig. 6(C) #4

epimerizations in which a stereoisogram of an epimeric correlation diagram (e.g., Stereoisogram #1 of Fig. 6(B): **5**→**6**) is combined with another stereoisogram of an appropriate main correlation diagram (e.g., Stereoisogram #2 of Fig. 6(C): **6**→**8**). Such a main correlation diagram and epimeric ones as shown in Table 3 are relative so that Fig. 6(B), (D), or (E) can be selected as a main correlation diagram in place of Fig. 6(C). The relative features in the selection of a main correlation diagram and in the appearance of stereoisograms can be extended to general cases.

Discussions based on such tables as Table 3 are sufficient to understand the total features of the stereoisomerism shown in Fig. 5. In order to show more clearly the over-simplified features of the traditional dichotomy between enantiomers and diastereomers, the fourteen diastereomeric relationships are translated into appropriate combinations of three *RS*-stereoisomeric relationships, among which *RS*-diastereomeric relationships and holantimeric ones are mainly

employed in Table 4.

The results shown in Table 4, which are derived from Table 3, can be confirmed by scrutinizing the stereoisomers shown in Fig. 5. For example, the conventional diastereomeric relationship between **5** and **8** (the pair-**5/8**-row of Table 4) is interpreted by a multiple process of epimerizations which correspond to two *RS*-diastereomeric relationships, as shown in the following scheme of conversion: **5** —(at C_2)→ **6** —(at C_3)→ **8**. Comparison between Table 3 and Table 4 shows that descriptions based on promolecules (Table 3) are more concise than those based on molecules (Table 4).

3.4 What Do *RS*-Descriptors Specify?

One of the most important conclusions is that *R* and *S*-descriptors of the CIP system are pairwise given to two promolecules in an *RS*-diastereomeric relationship. In other words, the capability of giving *RS*-descriptors is ascribed to local *RS*-stereogenicity. Although local *RS*-stereogenicity (corresponding to *RS*-diastereomeric relationships) and local chirality (corresponding to enantiomeric relationships) are closely linked with each other by means of a single stereoisogram, they are conceptually distinct.

In this context, the section title "Enantiomers: the CIP priority system" of IUPAC 2004 Provisional Recommendations [2, P-91] would cause undesigned confusion, because the CIP priority system has been clearly shown to deal with *RS*-diastereomers, not enantiomers. Because *RS*-diastereomers are linked with enantiomers to generate *RS*-stereoisomers by means of stereoisograms, a more plausible title would be "*RS*-Stereoisomers: the CIP priority system" or more definitely "*RS*-Diastereomers: the CIP priority system".

4 Conclusion

Correlation diagrams of stereoisograms have been developed to characterize a set of stereoisomers. Each of the stereoisomers is regarded as a tetrahedral uninuclear promolecule at an *RS*-stereogenic center or a binuclear promolecule at a bond selected to be considered. Stereoisograms, each of which contains a quadruplet of such promolecules, are collected to give a correlation diagram at the center or bond. When all of the *RS*-stereogenic centers (along with the bond) are taken into consideration, a set of correlation diagrams are generated to characterize the set of stereoisomers. Because each stereoisogram represents the local chirality/achirality and the local *RS*-stereogenicity/*RS*-astereogenicity of the *RS*-stereogenic center (or the bond), the corresponding correlation diagram indicates total features of such local symmetries. Thereby, over-simplified feature of the conventional dichotomy between enantiomers and diastereomers have been discussed in detail.

References

[1] IUPAC Organic Chemistry Division *Pure Appl. Chem.* **1996**, *68*, 2193–2222.

[2] IUPAC Chemical Nomenclature and Structure Representation Division *Provisional Recommendations. Nomenclature of Organic Chemistry* **2004**: *http://www.iupac.org/reports/provisional/abstract04/favre_310305.html*

[3] Morris, D. G. *Stereochemistry*; Royal Soc. Chem.: Cambridge, 2001.

[4] Mislow, K.; Siegel, J. *J. Am. Chem. Soc.* **1984**, *106*, 3319–3328.

[5] Fujita, S. *J. Org. Chem.* **2004**, *69*, 3158–3165.

[6] Fujita, S. *J. Math. Chem.* **2004**, *35*, 265–287.

[7] Fujita, S. *Tetrahedron* **2004**, *60*, 11629–11638.

[8] Fujita, S. *Chem. Educ. J.* **2005**, *8*, Registration No. 8–8.

[9] Fujita, S. *Tetrahedron* **1991**, *47*, 31–46.

[10] Fujita, S. *J. Chem. Inf. Comput. Sci.* **2000**, *40*, 426–437.

[11] Fujita, S. *J. Math. Chem.* **2008**, *43*, 141–201.

[12] Jordan, C. *J. Reine Angew. Math.* **1869**, *70*, 185–190.

[13] Cayley, A. *Philos. Mag.* **1874**, *47*, 444–446.

[14] Fujita, S. *Theor. Chem. Acc.* **2007**, *117*, 353–370.

[15] Fujita, S. *Theor. Chem. Acc.* **2007**, *117*, 339–351.

[16] Fujita, S. *Theor. Chem. Acc.* **2005**, *113*, 73–79.

[17] Fujita, S. *Theor. Chem. Acc.* **2005**, *113*, 80–86.

[18] Fujita, S. *Theor. Chem. Acc.* **2006**, *115*, 37–53.

[19] Fujita, S. *MATCH Commun. Math. Comput. Chem.* **2007**, *57*, 299–340.

[20] Jonas, J. *Coll. Czech. Chem. Commun.* **1988**, *53*, 2676–2714.

[21] Mislow, K. *Chirality* **2002**, *14*, 126–134.

[22] Mislow, K. *Introduction to Stereochemistry*; Benjamin: New York, 1965.

[23] Eliel, E.; Wilen, S. H. *Stereochemistry of Organic Compounds*; John Wiley & Sons: New York, 1994.

[24] North, N. *Principles and Applications of Stereochemistry*; Stanley Thornes: Cheltenham, 1998.

[25] Eliel, E. L.; Willen, S. H.; Doyle, M. P. *Basic Organic Stereochemistry*; Wiley-Interscience: New York, 2001.

[26] Black, K. A. *J. Chem. Educ.* **1990**, *67*, 141–142.

[27] Mislow, K. *Bull. Soc. Chim. Belg.* **1977**, *86*, 595–601.

[28] Vollhardt, K. P. C.; Schore, N. E. *Organic Chemistry. Structure and Function*, 4th ed.; Freeman: New York, 2003.

[29] Fujita, S. *Tetrahedron* **2006**, *62*, 691–705.

[30] Fujita, S. *Yuki Gosei Kagaku Kyokai-Shi/J. Synth. Org. Chem. Jpn.* **2008**, *66*, 995–1004.

[31] Fujita, S. *MATCH Commun. Math. Comput. Chem.* **2009**, *61*, 11–38.

[32] Fujita, S. *MATCH Commun. Math. Comput. Chem.* **2009**, *61*, 39–70.